JOURNAL OF GUIDANCE, CONTROL, AND DYNAMICS
Vol. 32, No. 3, May–June 2009

Designing Natural Formations of Low-Earth-Orbiting Satellites

Phil Palmer* and Mark Halsall
Surrey Space Centre, University of Surrey, Guildford, England GU2 7XH, United Kingdom

DOI: 10.2514/1.39631

In this paper, we describe possible natural formations for satellites in low Earth orbit that exploit the Earth's oblateness. These formations are based upon an analytic model of natural formations for satellites in nearly circular orbits, which has already been published, and explores the range of formations available. We describe how we parameterize the formations and then derive from this parameterization the orbital elements needed for each satellite orbit and then show the long-term evolution of these orbits to show the slow evolution of the formation geometry over time. We demonstrate that the formations maintain their projected shape in the sky without control over a day, in the presence of gravitational perturbations. This shows that the control requirements for long-term maintenance of such formations can be reduced considerably for long-term maintenance.

Nomenclature

a	=	semimajor axis of the guiding-center motion
a_k, I_{k0}, Ω_{k0}	=	differences in epicycle elements of satellite k and guiding center
e_k	=	eccentricity of orbit for satellite k
I	=	inclination of the guiding-center motion
R	=	equatorial radius of Earth
α_e, α_{Pk}	=	phase shift for equator crossing and perigee for satellite k
θ, κ	=	secular variations included in the guiding-center motion
τ	=	phase along the guiding-center orbit
ϕ_ϖ, ϕ_υ, ϕ_ζ	=	phases of oscillation in each curvilinear coordinate
χ	=	long-periodic variation evaluated for guiding-center orbit parameters
ϖ, υ, ζ	=	curvilinear coordinates of the sky with ϖ measuring depth
ϖ_F, υ_F, ζ_F	=	solid-body component to motion of formation
ϖ_M, υ_M, ζ_M	=	maximum variation in curvilinear coordinate by formation
ϖ_S, υ_S, ζ_S	=	internal component to motion of formation
ϖ_0, υ_0	=	center about which the satellite oscillates in curvilinear coordinates

I. Introduction

MANY planned missions are now beginning to take advantage of the benefits offered by the use of satellite formations. In addition to the generally lower cost associated with development and launch of smaller satellites, reduced risk of a mission-ending critical failure, and greater flexibility offered by the ability to reconfigure the formation, missions are being planned that can only be achieved by the use of multiple spacecraft. Among other objectives, the Gravity Recovery and Climate Experiment mission [1] uses a pair of satellites flying in formation in low Earth orbit (LEO) to make accurate gravitational measurements. Formation flight for a string-of-pearls formation has been demonstrated by the Space Technology 5 mission [2,3]. Increasing the complexity of the formation design from linear configurations, the Auroral Lites mission [4] uses four satellites in a tetrahedral pattern. The TerraSAR-X Add-On for Digital Elevation Measurement [5] mission will fly in close formation with the already-launched TerraSAR-X satellite to provide elevation measurements of the Earth's surface. TerraSAR-X is one of several missions proposed that use formation-flying satellites for synthetic aperture radar (SAR) [6,7]. In an extension to the SAR technique, Krieger et al. [8] consider an interferometric cartwheel using three satellites in formation to maintain a near-uniform radial baseline.

Much work on formation design has adopted the Hill–Clohessy–Wiltshire equations [9] used to model the approach to rendezvous and docking. This may be considered to be the limit of the epicycle model [10] when the geopotential is Keplerian. The advantage of using these equations is that they have a particularly simple form, and the out-of-plane motion decouples from the other directions. Sabol et al. [11] present a technique for designing satellite formations in this frame and use it to design a set of formations that are geometrically simple. They show how to determine initial conditions for each satellite to produce the formations. Among the formations they present is the projected circle formation. This paper is a natural extension of this work to other projected formations that exploit the Earth's oblateness.

In this paper, we focus upon the design of satellite formations in low Earth orbit, exploiting the natural dynamics to remove the need for station-keeping against the principal disturbing effects of Earth oblateness. The aim of the design process is to determine a set of orbital parameters for each of the satellites, so that the natural dynamics will approximately maintain a formation geometry under J_2 and J_3 terms. Higher-order terms are then treated as a disturbance to the formation, which require a much smaller control thrust. Such formations are of interest for observing the Earth and its environment. As a consequence, we shall pay particular attention to the projected geometries of the formation onto the plane of the sky. We assume that the satellites move on nearly circular orbits to remove the shearing effect experienced in more eccentric orbits. Lane and Axelrad [12] consider formation design for elliptic orbits. Their method uses orbital element differences in a similar way to this work, but is based on unperturbed Keplerian orbits.

Once the effects of Earth oblateness are incorporated, the problem of establishing formations and inverting the equations to find orbital parameters is more difficult. Guibout and Scheeres [13] present the problem of formation design when J_3 is incorporated into the dynamics as a boundary-value problem. Their approach aims to bring the satellites into a given configuration at a given time, rather than being in a given configuration over an extended period. This approach is therefore very different from the approach we adopt here.

II. Relative Epicycle Model

This paper uses the relative orbit model presented by the authors in [14,15], a relative motion model based on the epicycle orbit model developed by Hashida and Palmer [10,16]. The epicycle model

Received 8 July 2008; revision received 4 February 2009; accepted for publication 4 February 2009.

*P.Palmer@surrey.ac.uk (Corresponding Author).

describes orbits with small eccentricity and can incorporate all the geopotential terms and atmospheric drag. The position and velocity of the satellite are described using four coordinates to define the orbital plane and position and two components of velocity on the orbital plane. The four spatial coordinates r_k, λ_k, I_k, and Ω_k define the satellite position in an inertial frame. These are shown in Fig. 1. Associated with these coordinates is a set of orbital elements, or epicycle elements. These are defined as

$$\mathbf{x}_E = (a, e, I_0, \Omega_0, \alpha_P, \alpha_e)$$

where a and e are the orbital semimajor axis and eccentricity, I_0 and Ω_0 define the orbital plane at the instant of equator crossing at the chosen origin of time (note that the inclination and right ascension of ascending node (RAAN) will vary periodically and secularly over time), and α_P and α_e are the epicycle phases at the perigee passage and equator crossing. For a single satellite, we can choose the origin of time at equator crossing and set $\alpha_e = 0$. This is not possible, however, when considering a formation of satellites crossing the equator at different times.

The motion of a single satellite in the epicycle model, moving under the effects of J_2 and J_3, is given by

$$\begin{aligned} r &= a(1+\rho) - ae\cos(\tau - \alpha_P) + a\chi\sin\tau + \Delta_r\cos 2\tau \\ \lambda &= \tau(1+\kappa) + 2e[\sin(\tau-\alpha_P) - \sin\alpha_P] - 2\chi[1-\cos\tau] \\ &\quad + \Delta_\lambda \sin 2\tau \\ I &= I_0 + \Delta_I(1-\cos 2\tau) \qquad \Omega = \Omega_0 + \theta\tau + \Delta_\Omega \sin 2\tau \\ \tau &= nt \end{aligned} \tag{1}$$

where the secular variation due to J_2 is described by the terms θ and κ, the long-periodic effects of J_3 are given by χ, and the short-periodic effects by Δ_i.

The description of relative motion using these epicycle coordinates is defined with respect to a guiding center that moves on a circular orbit that secularly drifts due to the effects of J_2 on a satellite orbit. As there are no periodic terms involved in the motion of this guiding center, then no satellite can be placed on the origin and remain there over time. This choice is convenient, as it removes the principle secular effect on the formation while retaining all the periodic motions of the satellites. The position of the guiding center is also shown in Fig. 1, in which a subscript c is used to denote the coordinates defining its instantaneous orbital plane. The motion of each satellite in the formation can then be described relative to this guiding center by a set of epicycle elements:

$$\mathbf{x}_k = (\hat{a}_k, e_k, \hat{I}_{k0}, \hat{\Omega}_{k0}, \alpha_{Pk}, \alpha_e)$$

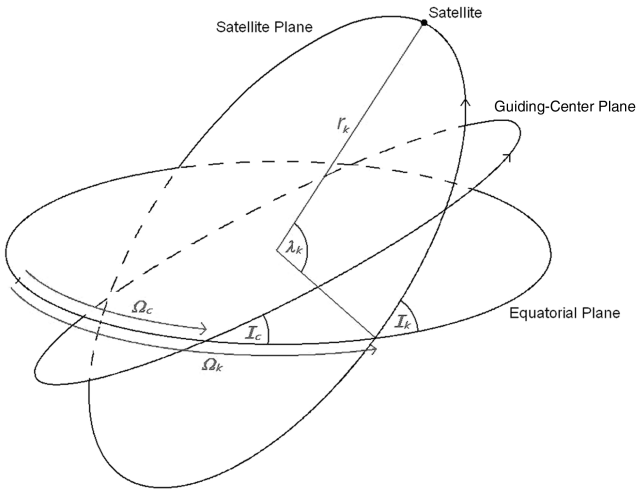

Fig. 1 Epicycle coordinates of one satellite and the guiding-center motion plane.

where k denotes the satellite in the formation. The caret denotes epicycle elements relative to the guiding center. There are relative secular drifts between these satellites and the guiding center, caused by J_2. As shown in [15], these differential drifts can be removed by adjusting the semimajor axes $\hat{a}_k$. Knowing the motion of the guiding center and these epicycle elements is enough to completely determine the motion of the satellite in inertial space.

The description of the relative motion described in [15] uses a curvilinear coordinate system (ϖ, υ, ζ), where ϖ denotes the difference in radial distance of the satellite and guiding center, and υ and ζ are defined on the celestial sphere, as shown in Fig. 2. This system is similar to that used in modeling proximity operations for the shuttle [17]. More details of the definitions of these coordinates and the motion of the satellite relative to the guiding center can be found in [15]. Because the guiding center moves on a perfectly circular orbit and we can fix our origin of time when this origin crosses the equator at an ascending node, then we need only three epicycle elements to define the motion of the guiding center: $\mathbf{x}_c = (a, I, \Omega_{c0})$. Note that Ω_c drifts secularly in time, and hence we use the instantaneous RAAN initially, but inclination is constant in time. The epicycle phase α defines where the guiding center is at any particular time along this orbit, where $\tau = nt$ and n is the mean motion associated with the guiding-center orbit.

The dynamic model for the motion of each satellite in the formation can be split into two separate parts: one that is common to all satellites in the formation (the solid-body motion) and a second that varies from satellite to satellite (the internal motions) [15]. The first part can be described by the expressions

$$\varpi_F = -a\chi\sin\tau + \frac{1}{4}J_2\left(\frac{R}{a}\right)^2 a\sin^2 I\cos 2\tau \tag{2}$$

$$\upsilon_F = 2\chi(\cos\tau - 1) + \frac{1}{8}J_2\left(\frac{R}{a}\right)^2 \sin^2 I\sin 2\tau \tag{3}$$

and

$$\zeta_F = -\frac{3}{4}J_2\left(\frac{R}{a}\right)^2 \sin 2I\sin\tau \tag{4}$$

where χ denotes the long-periodic effects of J_3, and R is the equatorial radius of the Earth. We consider the motion to be principally periodic with the orbital period and treat the terms at twice this frequency, as if they were smaller. This is reasonable for most inclinations. This describes the periodic way the formation moves around the guiding center, but it does so as a rigid configuration that does not distort. The other part of the motion describes the individual relative motions of satellites in the formation and so describes the changes in the formation geometry:

$$\varpi_S = \hat{a}_k - \theta a\sin I\hat{I}_{k0} - ae_k\cos[(1-\kappa)\tau - \alpha_{Pk}] \tag{5}$$

$$\begin{aligned} \upsilon_S &= -\alpha e(1+\kappa) + 2e_k\sin(\alpha_{Pk} - \alpha_e) + \hat{\Omega}_{k0}\cos I - \tfrac{1}{2}\hat{I}_{k0}\hat{\Omega}_{k0}\sin I \\ &\quad + 2e_k\sin[(1-\kappa)\tau - \alpha_{Pk}] \end{aligned} \tag{6}$$

$$\zeta_S = \hat{I}_{k0}\sec\Phi\sin[\tau - \Phi] \tag{7}$$

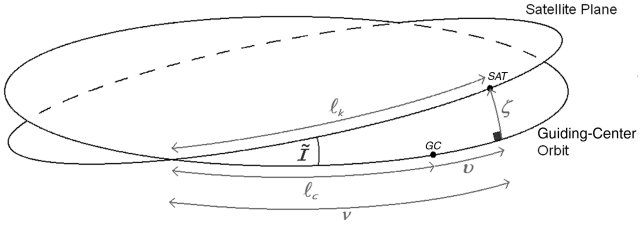

Fig. 2 Curvilinear coordinates for relative satellite positions.

where

$$\tan\Phi = \sin I(\hat{\Omega}_{k0} + \hat{\theta}_{k\tau})/\hat{I}_{k0} \tag{8}$$

The combination of these two components of the motion give a complete description of the satellites with respect to the guiding center, to the level of accuracy employed. Depending upon the application, we may not worry too much how the formation of satellites moves in the sky, as long as the geometric configuration is maintained. In this case, we only need to consider the second part of this motion described by Eqs. (5–8). For other applications, we may wish to keep the projected formation on the sky moving along a regular path, in which case, we would need to include both parts of the motion.

With this in mind, we note that Eqs. (5–8) can be written in the form

$$\varpi = \varpi_0 + \varpi_M \cos(\tau + \phi_\varpi) \tag{9}$$

$$\upsilon = \upsilon_0 + \upsilon_M \sin(\tau + \phi_\upsilon) \tag{10}$$

$$\zeta = \zeta_M \sin(\tau + \phi_\zeta) \tag{11}$$

where

$$\varpi_0 = \hat{a}_k - \theta a \sin I\hat{I}_{k0} \qquad \varpi_M = -ae_k \qquad \phi_\varpi = -\alpha_{Pk} - \kappa\tau \tag{12}$$

$$\upsilon_0 = -\alpha_e(1+\kappa) + 2e_k \sin(\alpha_{Pk} - \alpha_e) + \hat{\Omega}_{k0}\cos I - \tfrac{1}{2}\hat{I}_{k0}\hat{\Omega}_{k0}\sin I \tag{13}$$

$$\upsilon_M = 2e_k \qquad \phi_\upsilon = -\alpha_{Pk} - \kappa\tau \tag{14}$$

and

$$\zeta_M = \hat{I}_{k0}\sec\Phi \qquad \phi_\zeta = -\Phi \tag{15}$$

When we combine both parts of the motion, then we can still describe the motion in terms of Eqs. (9–11) as follows:

$$\varpi_0 = \hat{a}_k - \theta a \sin I\hat{I}_{k0} + \frac{1}{4}J_2\left(\frac{R}{a}\right)^2 a\sin^2 I\cos 2\tau \tag{16}$$

$$\varpi_M = a\sqrt{e_k^2 + \chi^2 + 2\chi e_k \cos(\alpha_{Pk} + \kappa\tau)} \tag{17}$$

$$\tan\phi_\varpi = -\frac{e_k \sin(\alpha_{Pk} + \kappa\tau)}{\chi + e_k\cos(\alpha_{Pk} + \kappa\tau)} \tag{18}$$

and

$$\upsilon_0 = -\alpha_e(1+\kappa) + 2e_k\sin(\alpha_{Pk} - \alpha_e) + \hat{\Omega}_{k0}\cos I - \frac{1}{2}\hat{I}_{k0}\hat{\Omega}_{k0}\sin I - 2\chi + \frac{1}{8}J_2\left(\frac{R}{a}\right)^2 \sin^2 I\sin 2\tau \tag{19}$$

$$\upsilon_M = 2\sqrt{e_k^2 + \chi^2 + 2\chi e_k \sin(\alpha_{Pk} + \kappa\tau)} \tag{20}$$

$$\tan\phi_\upsilon = \frac{\chi - e_k\sin(\alpha_{Pk} + \kappa\tau)}{e_k\cos(\alpha_{Pk} + \kappa\tau)} \tag{21}$$

and

$$\zeta_M^2 = \left(\hat{I}_{k0} - \frac{3}{4}J_2\left(\frac{R}{a}\right)^2 \sin 2I\right)^2 + \sin^2 I(\hat{\Omega}_{k0} + \hat{\theta}_k\tau)^2 \tag{22}$$

$$\tan\phi_\zeta = -\frac{\sin I(\hat{\Omega}_{k0} + \hat{\theta}_k\tau)}{\hat{I}_{k0} - \frac{3}{4}J_2(\frac{R}{a})^2\sin 2I} \tag{23}$$

These results show that in both cases, the motion can be described by the same equations, although the relationships between the preceding parameters and the orbital elements depend upon whether the whole motion is incorporated.

III. Design Parameters

The expressions for the relative motion can be described through the simple relations (9–11). If we consider the projection of this 3-D motion in the planes of any two of the local coordinates, then we obtain an ellipse. In particular, we are most interested in the projection of the motion onto the plane of the sky, which is the υ–ζ plane. We may exploit this simple geometric description to design formations of satellites with varying applications. In this section, we will define a set of design parameters that we have found useful in capturing the types of relative motion that may be exploited for differing formation designs.

The lack of any constant term in Eq. (11) means that the elliptic projection of the relative motion on the plane of the sky has its center along the υ axis. There is only one parameter required to determine where the center of the ellipse will be along this axis. We call this parameter c. This determines the distance from the center of the relative motion of one satellite with respect to the guiding center. Because the guiding center is a virtual reference point, we have the freedom to move it so that $c = 0$. When there are multiple satellites moving along different projected ellipses, then each ellipse will have a different value of c associated with it.

We may define two ellipse parameters for the semimajor and semiminor axes, a and b, and the orientation of the ellipse with respect to the υ axis, σ. Here, $(0 < \sigma < \pi)$. We require two further parameters: the first is φ, which determines the initial phase around the ellipse to place the satellite, and the second is d, which determines which way around the projected ellipse the satellite will appear to move. This last parameter takes the values of ± 1, where $+1$ implies that motion appears clockwise on the sky and -1 implies anticlockwise.

We illustrate this set of design parameters in Fig. 3, in which we show the projected ellipse as it would appear in the plane of the sky.

IV. Possible Configurations

We may now consider the design of formations of satellites based upon these design parameters, and in the following section, we shall

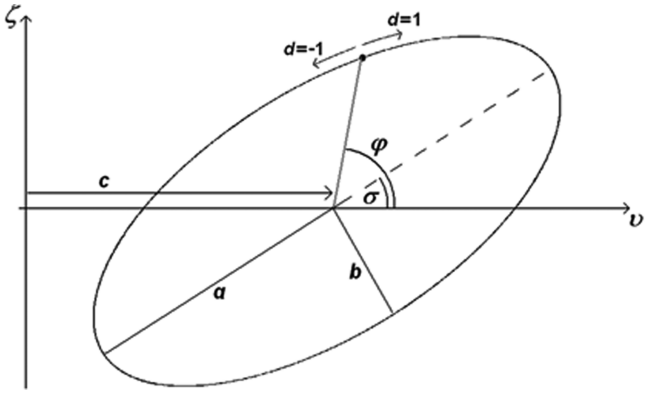

Fig. 3 Ellipse design parameters describing the relative motion of a satellite as seen in the plane of the sky.

review some of the formations that may be constructed using the natural control-free dynamics of LEO satellites. There is considerable flexibility in the choice of design parameters, and so we shall indicate only the nature of some of the more useful types of formations that can be created.

A. Leader–Follower

The simplest formation design is for a pair of satellites with one satellite following another along the same orbit. This would be equivalent to both satellites being on the same projected ellipse, so that only the parameter φ is different. In this case, we can fix $c = 0$ by a suitable choice of the guiding center. The baseline between the satellites varies as they move around the ellipse, and the maximum variation is obtained by separating them in phase by π. The baseline varies unless $a = b$, and the orientation varies according to σ.

Alternatively, the two satellites may be placed on separate projected ellipses, which allows for considerable variation in baseline length and orientation in the sky. If these two ellipses have $b = 0$ and $\sigma = 0$, then the baseline will be fixed in the υ direction and grow and shrink. In such a scenario, we may place one satellite on the guiding center and choose the parameters for the second satellite according to

$$a_2 = \tfrac{1}{2}(\ell_{\max} - \ell_{\min}) \tag{24}$$

$$c_2 = \tfrac{1}{2}(\ell_{\max} - \ell_{\min}) \tag{25}$$

The separation between these satellites now oscillates between $\ell_{\max}$ and $\ell_{\min}$, as shown in Fig. 4.

B. Fixed Rotating Configurations

If we fix $a = b$, then the projected ellipse becomes a circle. Satellites move around such circles at constant angular rates, with a period equal to the orbital period. If we select satellites to move on such projected circles with the same center, then we can choose $c = 0$; for a circle, σ has no meaning, and so may also be set it to zero. The satellites move in the same direction, and so d is fixed for all of them. By changing the phase φ and radius a of the projected circles, we can create regular patterns such as those described in Fig. 5. As the satellites move around the projected circles, the grid will rotate as a fixed pattern in the sky. Other more imaginative patterns can be created, such as those shown in Fig. 6.

C. Pulsating Configurations

It is possible to combine the geometry of the fixed configurations with the dynamic baseline of the leader–follower pair. To do this, we place satellites on projected ellipses that all have the same shape and center, but are rotated on the plane of the sky. In this case, we can again choose $c = 0$ and fix a, b, and d for all of the satellites. The values of σ and φ are chosen so that satellites sit in some geometric configuration, such as the circle shown in Fig. 7. In this example, we have chosen to distribute the ellipses in constant intervals in σ and placed two satellites on each projected ellipse. The angles φ are determined by the condition of being on the projected circle. As the satellites move around the projected ellipses, the circle diminishes in radius until reaching a minimum and then increases back to a maximum. The formation therefore pulsates in the sky.

If we allow satellites to move in the opposite sense around the projected ellipses, then we can increase the number of satellites per ellipse to four. The satellites do not collide, due to differences in the radial distance from Earth to maintain the formation. Such a configuration is shown in Fig. 8.

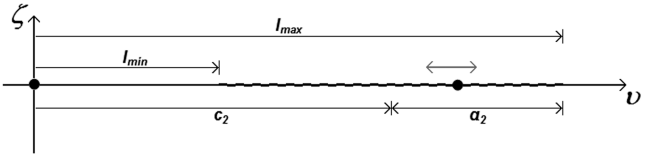

Fig. 4 Along-track linear formation.

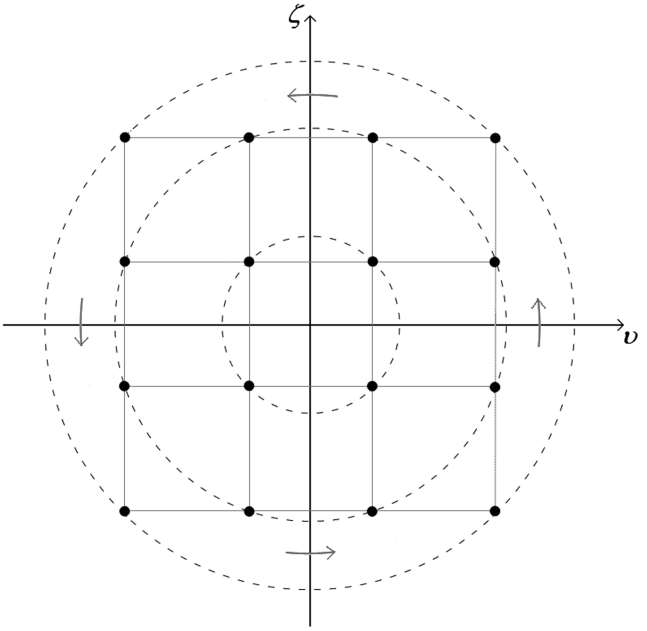

Fig. 5 Rotating grid formation. Dashed lines show the projected circles that the satellites appear to move around in the sky.

These formations exploit the symmetry by creating the same baseline lengths between corresponding pairs of satellites in the two ellipses, oriented differently on the sky. The effect is to make the baselines diameters of a pulsating circle on the sky. These baselines can be varied if we do not distribute the values of σ uniformly. The satellites still remain on the projected circles, but the baselines are more varied.

V. Determination of Required Orbital Elements

We now consider the problem of determining the orbital elements we require to generate the set of design parameter values we need to realize these formations. We break this into three stages: first to relate the design parameters $\mathbf{x}_D = (a, b, c, d, \sigma, \phi)$ to the parameters in

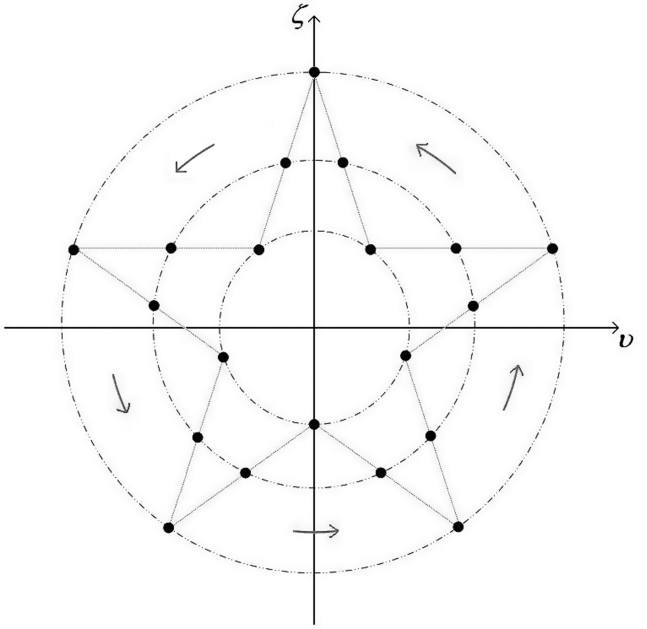

Fig. 6 This five-pointed star formation. Dashed lines show the projected circles that the satellites appear to move around in the sky.

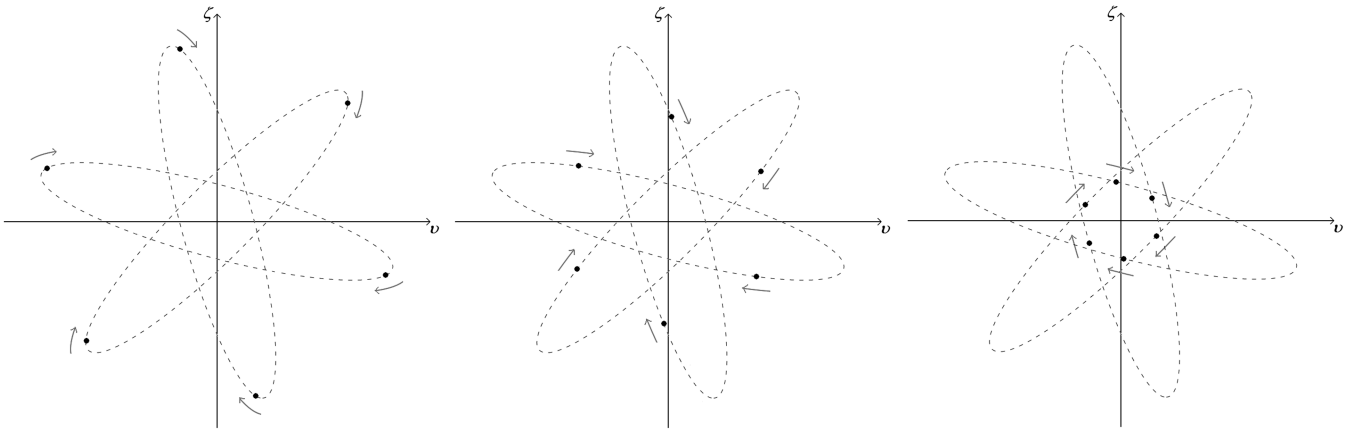

Fig. 7 Monodirectional varying-radius projected circle formation.

Eqs. (9–11), then we need to invert those equations to find the relative epicycle elements:

$$\mathbf{x} = (\hat{a}, e, \hat{I}_0, \hat{\Omega}_0, \alpha_P, \alpha_e)$$

Finally, from these elements and the parameters describing the motion of the guiding center, we can determine the absolute orbital elements required for each satellite.

We start by considering the relationship between the design parameters and the parameters in Eqs. (9–11). To this end, we consider the equation of the projected ellipse in the υ–ζ plane. This can be written as

$$\left(\frac{(\upsilon - c)\cos\sigma + \zeta\sin\sigma}{a}\right)^2 + \left(\frac{-(\upsilon - c)\sin\sigma + \zeta\cos\sigma}{b}\right)^2 = 1 \tag{26}$$

or expanding out, in the form

$$R(\upsilon - c)^2 + 2S(\upsilon - c)\zeta + T\zeta^2 = 1 \tag{27}$$

where

$$R = \left(\frac{\cos\sigma}{a}\right)^2 + \left(\frac{\sin\sigma}{b}\right)^2 \tag{28}$$

$$S = \sin\sigma\cos\sigma\left(\frac{1}{a^2} - \frac{1}{b^2}\right) \tag{29}$$

$$T = \left(\frac{\sin\sigma}{a}\right)^2 + \left(\frac{\cos\sigma}{b}\right)^2 \tag{30}$$

It is readily apparent that

$$\upsilon_0 = c \tag{31}$$

as this is the offset along the υ axis. We can find the parameters υ_M and ζ_M from the fact these are the limiting values of the υ and ζ coordinates around the ellipse. These may be found from Eqs. (27) by differentiating with respect to either υ or with respect to ζ and setting the derivatives to vanish. It is then straightforward to see that

$$\upsilon_M^2 = \frac{T}{RT - S^2} \tag{32}$$

and

$$\zeta_M^2 = \frac{R}{RT - S^2} \tag{33}$$

It is also readily shown from Eqs. (28–30) that $RT - S^2 = 1/(ab)^2$ and hence

$$\upsilon_M = (a^2\cos^2\sigma + b^2\sin^2\sigma)^{\frac{1}{2}} \tag{34}$$

$$\zeta_M = (a^2\sin^2\sigma + b^2\cos^2\sigma)^{\frac{1}{2}} \tag{35}$$

All that remains is to determine the phases ϕ and ϕ_ζ. To do this we need to consider the initial conditions. The value of τ is the time along the guiding-center motion, and $\tau = 0$ corresponds to the moment the guiding center crosses the equator at the ascending node. We may choose to arrange the formation at this time, but it may be more convenient to set the phases around the projected ellipse at some other time. We therefore suppose that the formation initial conditions are chosen at time τ_i. If the initial value of ζ is ζ_i, then

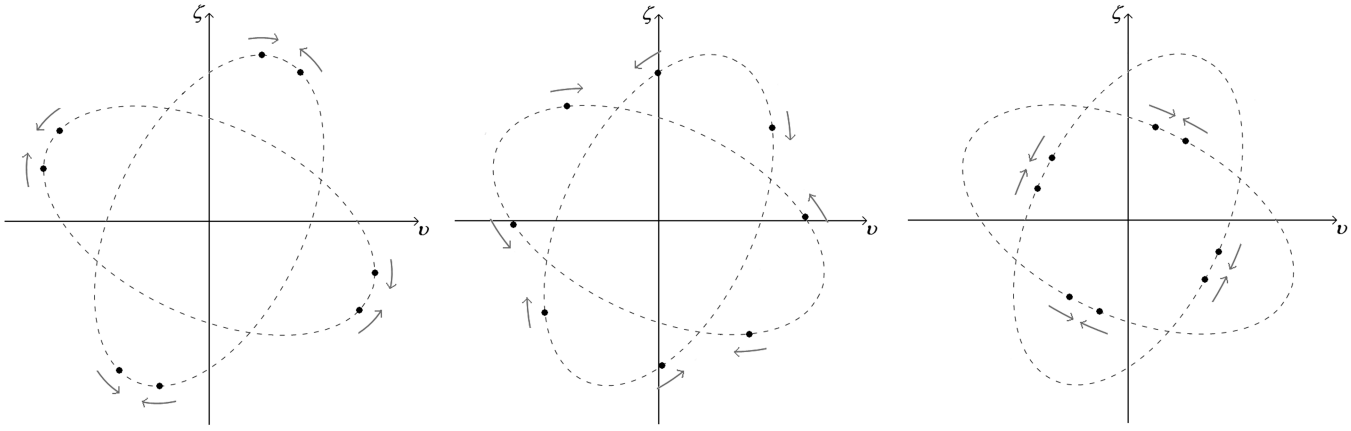

Fig. 8 Bidirectional varying-radius projected circle formation.

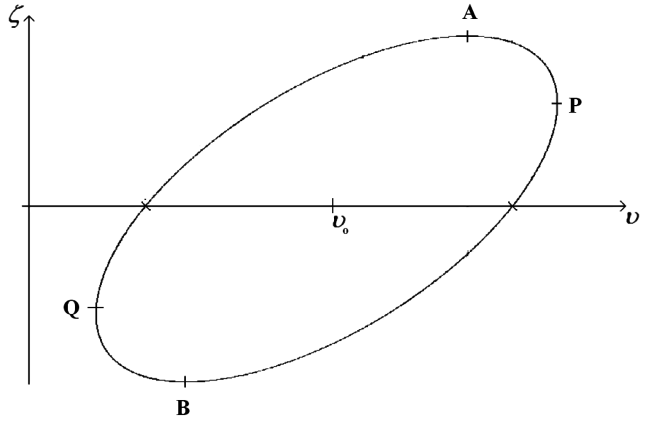

Fig. 9 Intermediate parameters and key points on ellipse for calculating orbital parameters.

$$\sin(\tau_i + \phi_\zeta) = \frac{\zeta_i}{\zeta_M} \tag{36}$$

There are two possible phases satisfying Eq. (36), which is resolved by the sign of $\dot{\zeta}_i$. Similarly, ϕ_υ can be determined from Eq. (10) as follows:

$$\sin(\tau_i + \phi_\upsilon) = \frac{\upsilon_i - c}{\upsilon_M} \tag{37}$$

To determine the signs of these derivatives, we split the projected ellipse into four arcs divided by the points A, B, P, and Q, as shown in Fig. 9. At the points A and B, $\zeta = \pm\zeta_M$, and at P and Q, $\upsilon = \pm\upsilon_M$. The signs of the derivatives are given in Table 1, in which the sign is related to the parameter d, determining whether the motion around the projected ellipse is clockwise or anticlockwise. The four points dividing the projected ellipse can be determined from the derivative:

$$\frac{d\zeta}{d\upsilon} = -\frac{R(\upsilon - c) + S\zeta}{S(\upsilon - c) + T\zeta} \tag{38}$$

and the numerator vanishes at A and B, whereas the denominator vanishes at P and Q. The signs of these expressions determine in which of the four arcs the initial conditions lie, as shown in Table 1.

A. Internal Satellite Motions

In the previous section, we inverted the design parameters to find the generic orbital parameters used in Eqs. (9–11). As described earlier, our formations can be designed so that the pattern moves as a whole with respect to the guiding center or they can be fixed with respect to the guiding center. In this section, we shall fix the internal motions of the individual satellites within the formation, but allow the formation to drift relative to the guiding center. In this case, we use expressions (13–15). Our purpose is to invert these expressions to find the individual satellite orbital elements: $\hat{I}_{k0}$, $\hat{\Omega}_{k0}$, α_{Pk}, e_k, $\hat{a}_k$, and α_e. As noted earlier, we can annul the differential secular drifts by fixing the relative semimajor axis of each satellite's orbit. In the case when only J_2 is considered, this gives [15]

$$\hat{a}_k = -2aJ_2\left(\frac{R}{a}\right)^2 \sin 2I\hat{I}_{k0} \tag{39}$$

where R is the equatorial Earth radius, and a and I are the orbital elements for the guiding center. For the other parameters, we can directly obtain the following:

$$e_k = \frac{\upsilon_M}{2} \tag{40}$$

$$\alpha_{Pk} = -\phi_\upsilon \tag{41}$$

$$\hat{I}_{k0} = \zeta_M \cos\phi_\zeta \tag{42}$$

From these results and Eq. (8), we obtain

$$\hat{\Omega}_{k0} = -\zeta_M \frac{\sin\phi_\zeta}{\sin I} - \hat{\theta}_k\tau_i \tag{43}$$

The last term accounts for the relative secular shift around the equator if we fix initial conditions at some other latitude. This just leaves α_e to be determined, which is now straightforward using Eq. (13), as all other terms are now known. This completes the inversion.

B. Using Complete Relative Motion

When we include the solid-body motion, then we need to invert Eqs. (19–23). In this case, from Eqs. (22) and (23), we can solve for $\hat{I}_{k0}$ and $\hat{\Omega}_{k0}$:

$$\hat{I}_{k0} = \zeta_M \cos\phi_\zeta + \frac{3}{4}J_2\left(\frac{R}{a}\right)^2 \sin 2I \tag{44}$$

and

$$\hat{\Omega}_{k0} = \zeta_M \frac{\sin\phi_\upsilon}{\sin I} - \hat{\theta}_k\tau_i \tag{45}$$

We next use Eqs. (20) and (21) to solve for e_k and α_{Pk}. To see how this is done, we introduce the variable $y = e_k \sin(\alpha_{Pk} + \kappa\tau_i)$. These equations can then be written as

$$(e_k^2 - y^2)\tan^2\phi_\zeta = (\chi - y)^2 \tag{46}$$

and

$$\tfrac{1}{4}\upsilon_M^2 - \chi^2 = e_k^2 + 2\chi y \tag{47}$$

We can eliminate the linear term in y between these to obtain

$$e_k^2 - y^2 = \tfrac{1}{4}\upsilon_M^2\cos^2\phi_\zeta \tag{48}$$

Table 1 ζ phase at numbered ellipse points

Arc	$\dot{\zeta}/\lvert\dot{\zeta}\rvert$	$\dot{\upsilon}/\lvert\dot{\upsilon}\rvert$	$R\upsilon + S\zeta$	$S\upsilon + T\zeta$
QA	d	d	<0	>0
AP	$-d$	d	>0	>0
PB	$-d$	$-d$	>0	<0
BQ	d	$-d$	<0	<0

Table 2 Formation design parameters for six-satellite varying-radius projected circle formation

Satellite	a, km	b, km	c, km	d	σ, deg	φ, deg
1	10.000	2.000	0.000	1	45.0	42.0
2	10.000	2.000	0.000	1	45.0	222.0
3	10.000	2.000	0.000	1	105.0	102.0
4	10.000	2.000	0.000	1	105.0	282.0
5	10.000	2.000	0.000	1	165.0	162.0
6	10.000	2.000	0.000	1	165.0	342.0

Table 3 Generalized elliptic motion parameters for six-satellite varying-radius projected circle formation

Satellite	υ_M, km	ζ_M, km	ϕ_υ, deg	ϕ_ζ, deg
1	7.211	7.211	93.37	115.99
2	7.211	7.211	−86.63	−64.01
3	3.230	9.673	−38.58	101.61
4	3.230	9.673	141.42	−78.38
5	9.673	3.230	−72.25	67.95
6	9.673	3.230	107.75	−112.05

Table 4 Relative epicycle parameters for six-satellite varying-radius projected circle formation using internal satellite motions only

Satellite	$\hat{a}_k$, m	$\hat{I}_k$, deg	$\hat{\Omega}_k$, deg	e_k	α_{Pk}, deg	α_e, deg
1	5.6813	−0.0259	−0.0750	0.000515	−93.3737	−0.1121
2	−5.6813	0.0259	0.0750	0.000515	86.6263	0.1121
3	3.5013	−0.0159	−0.1097	0.000231	38.5784	−0.0612
4	−3.5013	0.0159	0.1097	0.000231	−141.4216	0.0611
5	−2.1800	0.0099	−0.0346	0.000691	72.2489	0.0510
6	2.1800	−0.0099	0.0346	0.000691	−107.7511	−0.0509

Table 5 Relative epicycle parameters for six-satellite varying-radius projected circle formation using complete relative motions

Satellite	$\hat{a}_k$, m	$\hat{I}_k$, deg	$\hat{\Omega}_k$, deg	e_k	α_{Pk}, deg	α_e, deg
1	−2.8014	0.0128	−0.0750	0.001268	−91.3698	−0.1119
2	−14.1639	0.0645	0.0750	0.000241	−82.7803	0.1118
3	−4.9814	0.0227	−0.1097	0.000636	−73.5198	-0.0610
4	−11.9839	0.0546	0.1097	0.000915	−101.3640	0.0610
5	−10.6627	0.0485	−0.0346	0.000231	−24.3689	0.0508
6	−6.3027	0.0287	0.0346	0.001427	261.5117	−0.0509

Substituting this back into Eqs. (20) and (21) then results in

$$e_k^2 = \chi^2 + (\tfrac{1}{2}\upsilon_M)^2 - \chi\upsilon_M \sin\phi_\upsilon \tag{49}$$

and

$$\tan(\alpha_{Pk} + \kappa\tau_i) = \frac{\chi - \frac{1}{2}\upsilon_M \sin\phi_\zeta}{\frac{1}{2}\upsilon_M \cos\phi_\zeta} \tag{50}$$

Finally, α_e can be found from Eq. (19), as everything else is now known.

VI. Design Process

We now demonstrate the design process and computation of the orbital elements for individual satellites. This will then enable us to evaluate the accuracy of this methodology by propagating the resulting orbits forward and projecting onto the sky. For illustration, we have chosen to consider the varying-radius projected circle formation shown in Fig. 7. The formation design parameters for this are given in Table 2.

The first stage is to determine the parameters in Eqs. (9–11) for these satellites; $\upsilon_0 = 0$ for all satellites and the remaining parameters are given in Table 3.

These parameters are next converted into relative epicycle parameters using either internal satellite motions, as in Eqs. (5–8), or also incorporating the solid-body motion of the formation about the guiding center described by Eqs. (2–4). We show both sets of orbital parameters in Tables 4 and 5, respectively. These orbital parameters have been calculated based upon a guiding-center reference orbit with an inclination of 45 deg, semimajor axis of 7000 km, and right ascension of the ascending node of 0 deg.

These relative orbital parameters can now either be converted into absolute epicycle orbit parameters or propagated using the analytic epicycle orbit propagator described in [15]. The along-track and cross-track relative coordinates υ and ζ were then found using an exact transformation from the absolute epicycle coordinates to remove the guiding-center location. We start by considering the case when both the internal and solid-body motions are incorporated into the dynamic model. Propagating the six orbits for one day, we obtain the projected paths on the sky shown in Fig. 10. This shows that the pattern is well maintained, but each of the ellipses precesses slightly in the sky, and this will lead to some distortion of the pattern. This arises from a small frequency mismatch between the J_3 terms and the

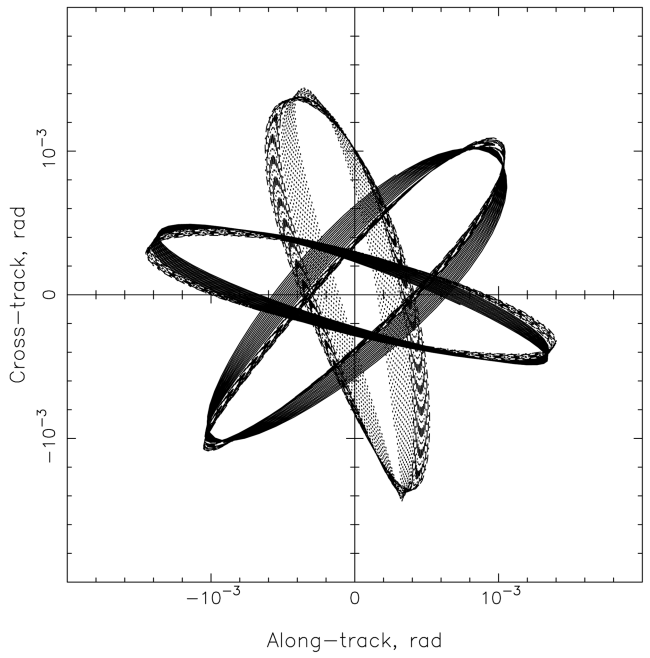

Fig. 10 Relative orbit paths for satellite formation designed using complete relative motions.

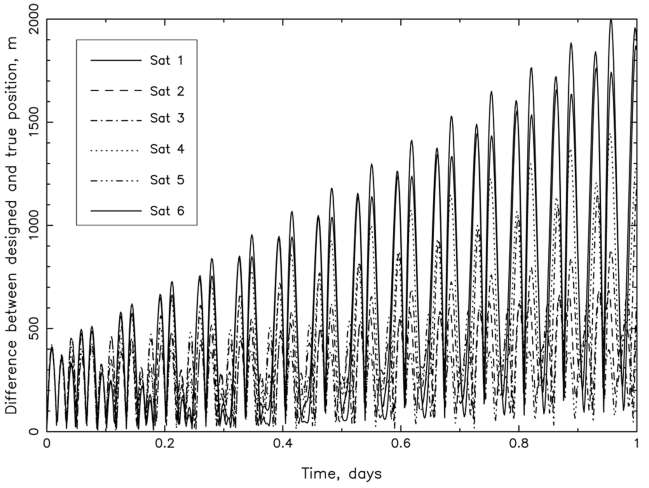

Fig. 11 Distance between satellite true position and ideal position for satellite formation designed using complete relative motions.

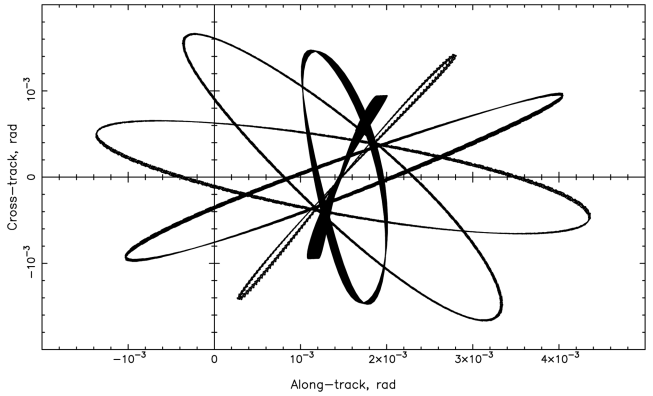

Fig. 12 Relative orbit paths for satellite formation designed using internal satellite motions only.

eccentricity terms. It is, of course, envisaged that any such formation would have active control to damp such drifts in formation geometry, but this shows that the level of required control is small, as the drift is much smaller than the size of the formation itself.

We can quantify the growth in errors over this propagation by comparing the propagated positions of the satellites with their locations in the ideal model used here. We show the variation of this positional error in Fig. 11, which shows that if unchecked, the position error grows to 2 km in one day. This is an upper estimate of the error, as the ellipses precess in the same sense in the plane of the sky, and so the relative errors in the geometry will be smaller.

Next, we consider the same formation geometry when we only consider the internal motions and allow the formation to drift with respect to the guiding center. We show the same propagation in this case in Fig. 12. This shows a more severe distortion from the expected geometry. This arises because we need to remove the guiding-center motion in the sky. This guiding-center motion may be modeled by propagating an orbit in which the relative epicycle parameters are zero (i.e., an orbit similar to that of the guiding center but in which periodic terms are also retained). Subtracting this motion from the motions of each of the six satellites shows a more regular pattern, as shown in Fig. 13. We note that the origin in this figure is no longer the guiding center, but is the center of the formation. We can clearly see that the desired configuration of satellites has been achieved. This figure shows that less control is

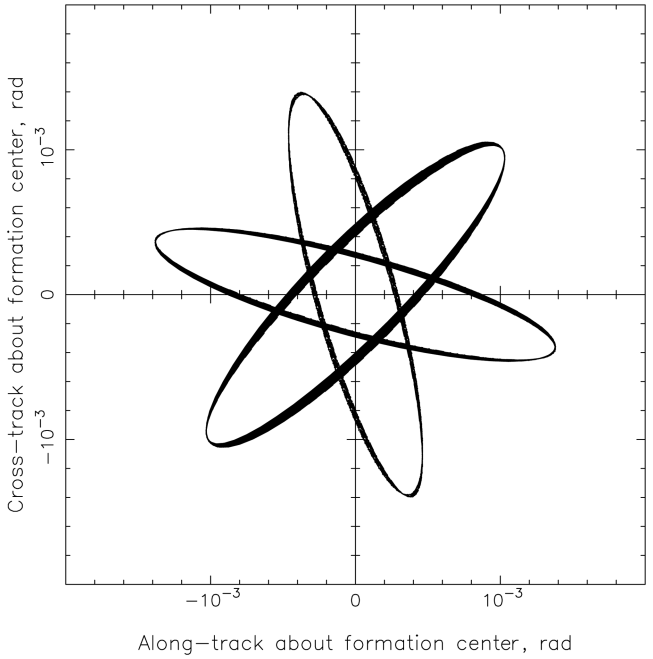

Fig. 13 Relative orbit paths once formation center motion has been subtracted.

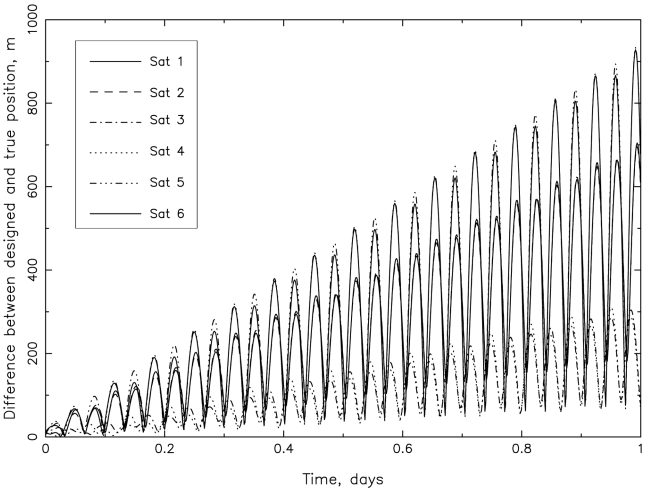

Fig. 14 Distance between satellite true position and ideal position for satellite formation designed using internal satellite motions only.

required to maintain the formation geometry. We may quantify this by propagating the difference between the ideal location and the propagated location of each of the six satellites. This is shown in Fig. 14.

The desired position is calculated on the assumption that each satellite remains on the design ellipse path, moving with an orbital period equal to the guiding-center orbital period. This deviation is periodic, depending upon position on the ellipse, and for the satellite with the largest deviation, it grows to approximately 900 m in one day. This deviation is not an error, but simply a result of the real dynamics when no control is applied. The position error is reduced by 45% when the pattern is allowed to oscillate with respect to the guiding center.

VII. Conclusions

In this paper, we have exploited an analytic model for the relative motion of satellites in near-circular low Earth orbits. This model conveniently separates the relative motion into a moving guiding center, which absorbs all the principal secular drift terms and periodic motion of satellites with respect to this guiding center. The periodic motion itself is further conveniently split between a rigid-body motion of the formation about the guiding center and individual satellite motions that change the geometry of the formation.

The analytic model gives a very simple description of the motions of these satellites projected onto the plane of the sky. The motion is described by a tilted ellipse. The parameters of these projected ellipses are directly related to the orbital elements of the satellites. A significant aspect of this analytic model is that these expressions can be inverted, and hence we can design satellite low-Earth-orbit formations based upon their projected geometry and then invert to determine what orbital parameters we require for each satellite. This makes for a powerful design tool for low-Earth-orbit constellations.

We have shown that a number of interesting geometries for low-Earth-orbit formations can be established in which a series of fixed baselines can be maintained or for pulsating formations in which the baseline varies periodically around the orbit. We have evaluated the formation geometry with direct simulation of the satellite orbits to show the rate of departure from the idealized geometry. This provides an indication of the level of orbital control that would be needed to maintain the formation geometry. Although this has not been formally evaluated using a control methodology, because we are exploiting the natural J_2 and J_3 dynamics of the geopotential, the control required is very affordable, even for small satellites with limited propellant capacity. We have demonstrated for one pulsating geometry that a 45% savings in propellant can be achieved if we allow the formation geometry to float with respect to the guiding center while maintaining the geometry of the formation.

Acknowledgment

The authors would like to acknowledge the support of the United Kingdom Engineering and Physical Sciences Research Council, who sponsored this research.

References

[1] Tapley, B. D., Bettadpur, S., Watkins, M., and Reigber, C., "The Gravity Recovery and Climate Experiment: Mission Overview and Early Results," *Geophysical Research Letters*, Vol. 31, No. 9, May 2004, Paper L09607. doi:10.1029/2004GL019920

[2] Speer, D., Jackson, G., Stewart, K., and Hernandez-Pellerano, A., "The Space Technology 5 Avionics System,"*IEEE Aerospace Conference*, Inst of Electrical and Electronics Engineers, Piscataway, NJ, Mar. 2005, pp. 768–780.

[3] Slavin, J. A., Carlisle, C. C., and Webb, E. H., "Space Technology 5: Changing the Mission Design Without Changing the Hardware," *IEEE Aerospace Conference*, Inst of Electrical and Electronics Engineers, Piscataway, NJ, Mar. 2005, pp. 758–767.10.1109/AERO. 2005.1559368

[4] Hametz, M. E., Conway, D. J., and Richon, K., "Design of a Formation of Earth Orbiting Satellites: The Auroral Lites Mission," *1999 NASA/ GSFC Flight Mechanics Symposium*, NASA, Greenbelt, MD, 1999, pp. 295–308.

[5] Krieger, G., Moreira, A., Fiedler, H., Hajnsek, I., Werner, M., Younis, M., and Zink, M., "TanDEM-X: A Satellite Formation for High-Resolution SAR Interferometry," *IEEE Transactions on Geoscience and Remote Sensing*, Vol. 45, No. 11, Pt. 1, Nov. 2007, pp. 3317–3341. doi:10.1109/TGRS.2007.900693

[6] Gill, E., and Runge, H., "Tight Formation-Flying for an Along-Track SAR Interferometer," *Acta Astronautica*, Vol. 55, Nos. 3–9, 2004, pp. 473–485. doi:10.1016/j.actaastro.2004.05.044

[7] Moccia, A., Vetrella, S., and, Bertoni, R., "Mission Analysis and Design of a Bistatic Synthetic Aperture Radar on Board a Small Satellite," *Acta Astronautica*, Vol. 47, No. 11, 2000, pp. 819–829. doi:10.1016/S0094-5765(00)00137-5

[8] Krieger, G., Zink, M., and Amiot, T., "Interferometric Performance of a Cartwheel Constellation for TerraSAR-l," *FRINGE 2003 Workshop* [CD-ROM], ESA SP-550, ESA European Space Research Inst., Frascati, Italy, Dec. 2003.

[9] Clohessy, W. H., and Wiltshire, R. S., "Terminal Guidance System for Satellite Rendezvous," *Journal of the Aerospace Sciences*, Vol. 27, No. 9, 1960, pp. 653–658, 674.

[10] Hashida, Y., and Palmer, P., "Epicyclic Motion of Satellites About an Oblate Planet," *Journal of Guidance, Control, and Dynamics*, Vol. 24, No. 3, 2001, pp. 586–596. doi:10.2514/2.4750

[11] Sabol, C., Burns, R., and McLaughlin, C. A., "Satellite Formation-Flying Design and Evolution," *Journal of Spacecraft and Rockets*, Vol. 38, No. 2, 2001, pp. 270–278. doi:10.2514/2.3681

[12] Lane, C., and Axelrad, P., "Formation Design in Eccentric Orbits Using Linearized Equations of Relative Motion," *Journal of Guidance, Control, and Dynamics*, Vol. 29, No. 1, 2006, pp. 146–160. doi:10.2514/1.13173

[13] Guibout, V. M., and Scheeres, D. J., "Spacecraft Formation Dynamics and Design," *Journal of Guidance, Control, and Dynamics*, Vol. 29, No. 1, 2006, pp. 121–133. doi:10.2514/1.13002

[14] Halsall, M., and Palmer, P. L., "An Analytic Relative Orbit Model Incorporating J3," AIAA/AAS Astrodynamics Specialist Conference and Exhibit, Keystone, CO, AIAA Paper 2006-6761, 2006.

[15] Halsall, M., and Palmer, P. L., "Modeling Natural Formations of LEO Satellites," *Celestial Mechanics and Dynamical Astronomy*, Vol. 99, No. 2, 2007, pp. 105–127. doi:10.1007/s10569-007-9084-7

[16] Hashida, Y., and Palmer, P., "Epicyclic Motion of Satellites Under Rotating Potential," *Journal of Guidance, Control, and Dynamics*, Vol. 25, No. 3, 2002, pp. 571–581. doi:10.2514/2.4919

[17] Adamo, D., "A Meaningful Relative Coordinate System for Generic Use," AIAA/AAS Astrodynamics Specialist Conference, Lake Tahoe, NV, American Astronautical Society Paper 05-306, 2005.